View metadata, citation and similar papers at core.ac.uk

brought to you by CORE

provided by Cronfa at Swansea University

Cronfa - Swansea University Open Access Repository

This is an author produced version of a paper published in :
Annals of the BMVA

Cronfa URL for this paper:
http://cronfa.swan.ac.uk/Record/cronfa20959

Paper:
Zhao, F. & Xie, X. (2013). An Overview on Interactive Medical Image Segmentation. *Annals of the BMVA*(7), 1-22.

http://dx.doi.org/doi=10.1.1.413.2364

This article is brought to you by Swansea University. Any person downloading material is agreeing to abide by the terms of the repository licence. Authors are personally responsible for adhering to publisher restrictions or conditions. When uploading content they are required to comply with their publisher agreement and the SHERPA RoMEO database to judge whether or not it is copyright safe to add this version of the paper to this repository.
http://www.swansea.ac.uk/iss/researchsupport/cronfa-support/

Annals of the BMVA Vol. 2013, No. 7, pp 1–22 (2013)

An Overview on Interactive Medical Image Segmentation

Feng Zhao and Xianghua Xie

Department of Computer Science,
Swansea University, Swansea SA2 8PP, UK
⟨f.zhao@swansea.ac.uk, x.xie@swansea.ac.uk⟩

Abstract

Image segmentation is often described as partitioning an image into a finite number of semantically non-overlapping regions. In medical applications, it is a fundamental process in most systems that support medical diagnosis, surgical planning and treatments. Generally, this process is done manually by clinicians, which may be time-consuming and tedious. To alleviate the problem, a number of interactive segmentation methods have been proposed in the literature. These techniques take advantage of automatic segmentation and allow users to intervene the segmentation process by incorporating prior-knowledge, validating results and correcting errors, thus potentially lead to accurate segmentation results. In this paper, we present an overview on interactive segmentation techniques for medical images.

1 Introduction

Due to the restrictions imposed by image acquisition, pathology, and biological variation, the medical images captured by various imaging modalities such as X-ray computed tomography (CT) and magnetic resonance imaging (MRI) are generally of high complexity and ambiguity. Image segmentation is typically used to locate objects of interest and their boundaries to make the representation of a volumetric image stack more meaningful and easier for analysis. Traditionally, this process is manually done slice by slice, which requires expert knowledge to obtain accurate boundary information for the regions of interest. This editing process may take a lot of time as well. A number of computer-aided segmentation techniques have been developed for medical images, which can usually be distinguished as automatic (unsupervised), interactive (semi-supervised), and supervised methods.

Supervised segmentation methods [Hansen and Higgins, 1997, Reyes-Aldasoro and Bhalerao, 2007, Olivier et al., 2008, Schaap et al., 2011] require manually labelled training data for detecting specific objects in images, which may limit the scope of these methods. Unsupervised (automatic) methods (e.g., thresholding [Smith et al., 2007], watershed [Grau et al., 2004], edge detection [Mondal et al., 2011], morphological operation [Kubota et al., 2011], neural

© 2013. The copyright of this document resides with its authors.
It may be distributed unchanged freely in print or electronic forms.

network [Pitiot et al., 2002], region growing [Wu et al., 2008a], and shape analysis [Diciotti et al., 2011]) provide segmentation results without prior-knowledge about the images and do not require user interaction. These methods are usually applicable for the segmentation of well-circumscribed objects. When applied to a stack of medical images, they are able to generate rough segmentation results. These results can be further refined by the intervention of human experts. In computer-aided diagnosis, therapy planning and treatment, interactive segmentation [Kass et al., 1988, Boykov and Jolly, 2001, Yeo et al., 2011] has become more and more popular in recent years, as the combination of human experts and machine intelligence can provide improved segmentation accuracy and efficiency with minimal user intervention [Lee et al., 2008]. The improved segmentation results can be used to reconstruct the 3D structures of tissues and enhance the real-time visualisation on the screen for clinicians to navigate through the data. This can provide great benefits to many applications including locating tumours, measuring tissue volumes, surgery, and diagnosing diseases.

In this overview, we will focus on the interactive segmentation methods popular for medical image analysis. Our goal is to better understand the implications of user interaction for the design of interactive segmentation methods and how they affect the segmentation results. The remainder of this paper is organised as follows. In Section 2, we present the interactive segmentation methodologies including fundamental approaches, learning-based approaches, and energy minimisation-based approaches. The variety of user interactions in medical image segmentation are given in Section 3. In Section 4, we explain the criteria for the evaluation of the overall segmentation quality and give examples for the comparison of the segmentation results by different methods. We finally conclude this paper in Section 5.

2 Interactive Segmentation Methodologies

Interactive segmentation [Olabarriaga and Smeulders, 1997, Smeulders et al., 1997] plays an important role in the segmentation of medical images, where user intervention is suggested as an additional source of information. This technique leverages the expert knowledge of users to produce accurate segmentation of anatomical structures, which facilitates measurement and diagnosis of various diseases. Many approaches have been taken in interactive segmentation, which can be broadly classified into the following categories.

2.1 Fundamental approaches

In this section, we will review some common techniques (e.g., level set, region growing) that are used in interactive segmentation of medical data (see Fig. 1).

Edge-based and region-based level set segmentation methods provide a direct way to estimate the geometric properties of anatomical structures. They are popular as a general framework for many applications of medical image analysis [Baillard and Barillot, 2000, Cremers et al., 2007b], such as brain MRI images and 3D CT of carotid arteries. Region growing [Adams and Bischof, 1994] is a simple region-based interactive segmentation method. Several variants of this technique have been proposed for medical image segmentation, e.g., the adaptive region growing algorithm introduced in [Wu et al., 2008b]. They perform well with respect to noise and usually produce good segmentation results. However, these techniques may result in holes or over-segmentation due to noise or variation of intensity.

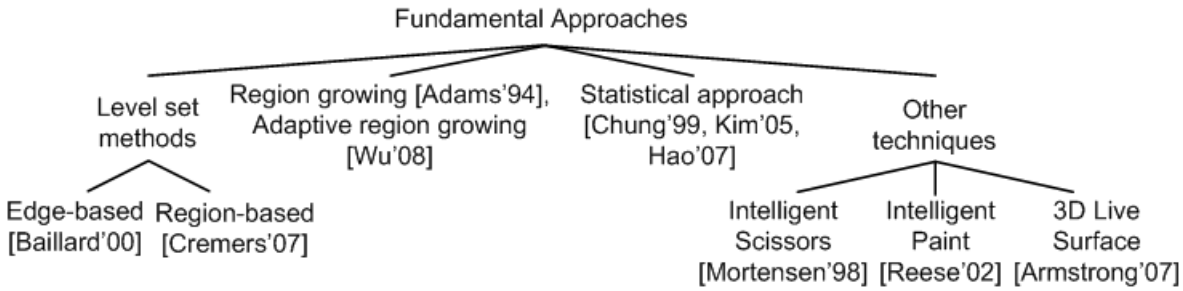

Figure 1: The hierarchical taxonomy of fundamental interactive segmentation methods.

Statistical approach [Hao and Li, 2007] is also applied to identify different tissue structures from medical images, which involves manual interaction to segment images in order to obtain a sufficiently large set of training samples. This technique is mainly applicable for problems with sufficient prior knowledge about the shape or appearance variations of the relevant structures [Chung and Noble, 1999, Kim et al., 2005]. Mortensen and Barrett [Mortensen and Barrett, 1998] developed an effective graphical tool (intelligent scissors) for performing 2D segmentation by providing immediate feedback for boundary selection as the mouse moves, which gives the user constant awareness of what belongs to the current selection. Other graph-based segmentation tools include region-based intelligent paint [Reese and Barrett, 2002] and 3D live surface [Armstrong et al., 2007].

2.2 Learning-based approaches

As illustrated in Fig. 2, this interactive strategy can react dynamically to the user based on the input priors (e.g., shape and appearance), and then refine the segmentation results for the user. In this framework, the user only needs to label the foreground and background on a single volumetric data, the algorithm learns the correlation between them adaptively, and completes the segmentation on other volumetric data automatically. The goal is to improve the performance of the computational part and possibly reduce the need for future user intervention, leading to interaction efficiency.

In the method described by Elliot et al. [Elliot et al., 1992], the segmentation result obtained with user interaction is compared to the result obtained when the default parameter settings are used. The difference between the two is used to calibrate the parameters for the computational part, which are used as default values in future segmentation sessions. In slice-by-slice segmentation of 3D images, the information obtained with interaction in one slice can be propagated to the next in different ways. In [Sijbers et al., 1996], all the pixels inside the resulting object are propagated as seeds for region growing in the next slice. In the active paintbrush [Maes, 1998], selected points inside and outside the resulting object are propagated as 'hint' that indicates regions in the next slice where the object should (or should not) be located. The interactive method described in [Cagnoni et al., 1999] uses a set of reference contours drawn by the user to find the optimal parameters for an elastic-contour model using a genetic algorithm. The optimised parameters are used in all the other slices in the same or another dataset. In Yu's method [Yu and Yla-Jaaski, 1996], the resulting boundary itself is propagated as the initial contour for deformation in the next slice. In the method by Wink et al. [Wink et al., 1997], the contour in the next slice is estimated on the basis of local similarity measures of the image intensity pattern at the resulting boundary.

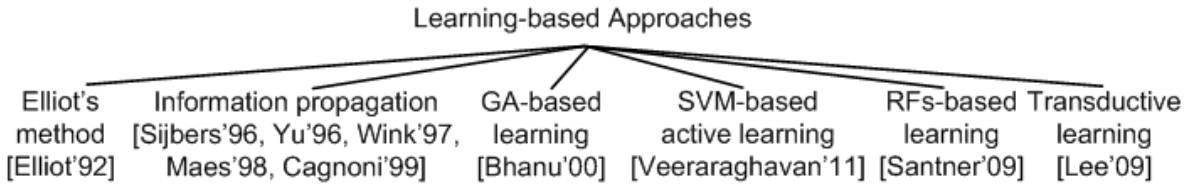

Figure 2: Learning-based interactive segmentation methods.

To overcome the application dependency, Bhanu and Fonder [Bhanu and Fonder, 2000] proposed a learning-based interactive segmentation approach, in which the user can select sets of examples and counter-examples to interactively train the segmentation. The image segmentation is guided by a genetic algorithm that learns the appropriate subset and spatial combination of a collection of discriminative functions, associated with image features. The genetic algorithm encodes the discriminative functions into a functional template representation, which can be applied to the input image to produce a segmentation result. In [Veeraraghavan and Miller, 2011], Veeraraghavan and Miller combined SVM-based active learning with GrowCut interactive segmentation to achieve a robust segmentation despite user variability with a comparable accuracy to a fully user guided segmentation with half number of user interactions on average. In [Santner et al., 2009], Santner et al. applied an online Random Forests (RFs) [Breiman, 2001, Saffari et al., 2009] to predict the labels of foreground and background pixels by learning complex pixel descriptors extracted from Gaussian smoothed images. The RF classifier is a set of multiple random decision trees. Each tree is trained by the training set randomly selected from the entire training set, and it consists of two types of nodes: split nodes and leaf nodes. In order to find an appropriate decision function for a split node, a set of random functions is generated and evaluated on every sample at that node. The one maximising the gain of information is selected as the best classifier at that node. The process continues recursively at each split node until reaching a leaf node. A leaf node is created when the tree depth is reached or no gain of information is achieved if a split happens. Associated with every leaf node is the probabilities for all the classes at that node.

The lack of labelled multimodal medical image data is a major obstacle for devising learning-based interactive segmentation tools. Transductive learning (TL) or semi-supervised learning offers a workaround by leveraging unlabelled and labelled data to infer labels for the test set given a small portion of label information. Lee et al. [Lee et al., 2009] proposed a novel algorithm for interactive segmentation using TL and inference in conditional mixture naive Bayes models (T-CMNB) with spatial regularisation constraints. T-CMNB is an extension of the transductive naive Bayes algorithm to the semi-nonparametric case, and the naive conditional independence assumption allows efficient inference of marginal and conditional distributions for large scale learning and inference.

2.3 Energy minimisation-based approaches

This class of segmentation methods partitions an image into different regions based on energy minimisation. Here, *energy* is a cost function measuring the variation within a labelling and the disagreement between the labelling and the observed data. Among many other approaches, graph cut-based methods and deformable model-based methods are particularly popular in medical image segmentation. These techniques aim to find a global or local solution for the boundary and region segmentation of objects in images and their performance

can be efficiently improved by involving users in the process at the time minimising user input.

2.3.1 Graph cut-based approaches

Based on combinatorial optimisation, graph cut [Shi and Malik, 2000, Boykov and Jolly, 2001] approaches the segmentation problem by minimising an energy function defined on a combination of both region and boundary terms. In this approach, a graph is composed of vertices representing image pixels or voxels, and edges connecting the vertices. The graph edges are assigned some nonnegative weights or costs, and a cut is a subset of edges that partition the vertices into disjoint sets. The cost function consists of both regional and boundary information, which needs to be well defined to provide a globally optimal solution. Many current techniques use graph cut for image segmentation. It has been shown to be effective in the segmentation of images [Li et al., 2004, Rother et al., 2004] and volumes [Armstrong et al., 2007]. The use of graph cut for segmentation of 3D surfaces has been extensively validated for medical image volumes [Li et al., 2006b]. However, the execution time can be tens of minutes to cut volumes of 2-8M voxels. To accelerate the process, a single layer of oversegmentation regions has been used in the place of voxels for medical volumes which reduces the computation time to tens of seconds [Yuan et al., 2005]. Lombaert et al. [Lombaert et al., 2005] used a resolution pyramid to perform coarse-to-fine refinement, enabling computation on the order of tens of seconds as well. In these techniques, the users are involved in the process by roughly marking out the objects of interest and the background before applying the graph cut-based segmentation. By using instant feedback, additional user interaction is specified to refine the results.

2.3.2 Deformable model-based approaches

Based on variational framework, deformable modelling [Kass et al., 1988, Caselles et al., 1993, Malladi et al., 1995, Eviatar and Somorjai, 1996] segments images by minimising an energy function defined on a continuous contour or surface. It can adapt to complex shape variations and incorporate priors to regularise segmentation. Deformable modelling has been widely applied in applications such as shape extraction and object tracking, in which curves or surfaces evolve under the influence of both internal and external forces to extract the object boundaries.

Explicit models such as active contour models (snakes) [Kass et al., 1988, Eviatar and Somorjai, 1996] represent contours or surfaces in their parametric form during deformation, which have the ability to track the points on the curves or surfaces across time, and are suitable for real-time applications. However, they generally have difficulties in handling topological changes due to the parameterisation of the curves or surfaces. To address these limitations, McInerney and Terzopoulos [McInerney and Terzopoulos, 1999] developed topology adaptive deformable models by formulating deformable surfaces in terms of an affine cell image decomposition to deal with topological changes usually existing in medical image volumes. This explicit model requires a periodic reparameterisation mechanism to manage complex shapes and changes in topology. This technique can effectively segment complex anatomic structures from medical volume images. However, it only performs well when the model is required to inflate or deflate everywhere, which limits its applications. Other approaches [Delingette and Montagnat, 2001, Bredno et al., 2003, Lauchaud and Taton, 2005]

have been proposed to handle topological changes. These techniques generally involve a set of heuristic algorithms to detect self-intersections and handle splitting and merging of the deforming grid, which can be computationally expensive. In addition, they may not work well on structures consisting of complex topologies.

To address the limitations of explicit deformable models, implicit deformable models [Caselles et al., 1993, Malladi et al., 1995] are introduced, based on the theory of curve evolution and the level set method [Osher and Sethian, 1988, Sethian, 1999]. In the implicit models, the evolution of curves or surfaces is implicitly represented as a level set of a higher dimensional scalar function and the deformation of the models is based on geometric measures such as the unit normal and curvature. Thus, the evolution is independent of the parameterisation and topological changes such as splitting and merging can be handled automatically. Implicit deformable models have been widely used in the segmentation of anatomical structures from 3D medical images [Baillard and Barillot, 2000, Holtzman-Gazit et al., 2006, Law and Chung, 2009].

Deformable models often vary in the object boundary representation and external force field used. Previous approaches can be distinguished as gradient-based methods [Malladi et al., 1995, Xu and Prince, 1998b, Paragios et al., 2004, Li et al., 2005, Xie and Mirmehdi, 2008], region-based methods [Chan and Vese, 2001, Paragios and Deriche, 2002, Vese and Chan, 2002, Kim et al., 2005, Cremers et al., 2007b], and hybrid methods [Kimmel, 2003, Xie and Mirmehdi, 2004]. Gradient-based techniques have been found useful when there is limited prior knowledge and image gradients are reasonable indications of object boundaries. However, they require careful initialisation and it may be difficult for them to achieve initialisation invariance and robust convergence. This is especially true when segmenting objects with complex geometries and shapes in 3D images. Notably, Xie in [Xie, 2010] presented an initialisation-invariant edge-based active contour model, which provides great freedom in contour initialisation. Region-based techniques have been widely applied to image segmentation as well. In the popular approach [Chan and Vese, 2001], Chan and Vese assumed the image consists of regions of approximately piecewise-constant intensities, and then extracted the objects based on the average intensities inside and outside the contour. This method is useful for the extraction of objects with smoothly varying boundaries. However, it has difficulties dealing with image regions with intensity inhomogeneity. Other region-based approaches also assumed that the image objects are composed of distinct regional features. This is usually not true for real images due to intensity inhomogeneity and multimodal nature. In the hybrid approach [Kimmel, 2003], Kimmel used image gradient vector directions as an alignment measure, combined with the geodesic active contour and minimal variance criterion [Chan and Vese, 2001]. The alignment measure is used to optimise the orientation of the curve with respect to the image gradients. This measure, together with the gradient-based geodesic measure and the region-based minimal variance criterion is then used to push or pull the contour towards the image boundary. However, this hybrid technique requires careful tuning of the different parameters associated with various measures in order to efficiently bridge the image gradient and regional information. In addition, only local edge information is used in the alignment measure, while edge information of pixels located away from the contour is not considered.

As shown in Fig. 3, the geometric active contour model [Caselles et al., 1993, Malladi et al., 1995] and subsequent geodesic active contour model [Caselles et al., 1997, Siddiqi et al., 1998] are two early deformable models for image segmentation. However, they have difficulties in handling the boundary concavities, weak edges and image noise. The generalised

Annals of the BMVA Vol. 2013, No. 7, pp 1–22 (2013)

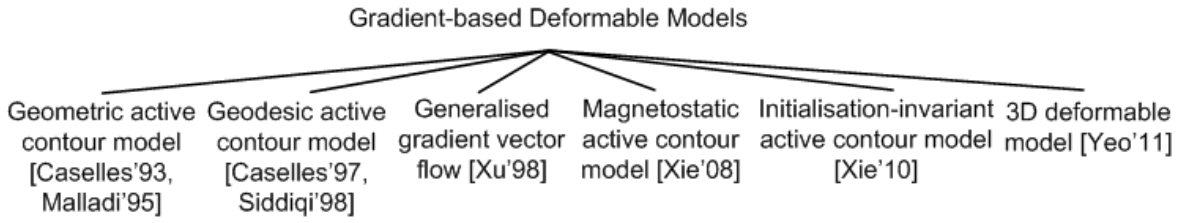

Figure 3: Gradient-based deformable modelling.

gradient vector flow [Xu and Prince, 1998a,b] achieves some improvements but has convergence issues caused by saddle or stationary points in its force field. In [Xie and Mirmehdi, 2008, Xie, 2010], Xie and Mirmehdi presented a novel edge-based model where the introduced external force field is based on the hypothesised magnetic force between the active contour and object boundaries. This method shows significant improvements in handling weak edges, broken boundaries, and complex geometries. However, its analogy based on magnetostatics cannot be directly applied to 3D or higher-dimensional images. Recently, Yeo et al. proposed a novel 3D deformable model [Yeo et al., 2011] based on a geometrically induced external force field, which is called the geometric potential force (GPF) field as it is based on the hypothesised interactions between the relative geometries of the deformable model and the object boundary characterised by image gradients. The evolution of the deformable model is solved using the level set method so as to facilitate topological changes automatically. The bi-directionality of the proposed GPF field allows the new deformable model to deal with arbitrary cross-boundary initialisations, which is very useful in the segmentation of complex geometries, and facilitates the handling of weak image edges and broken boundaries. Moreover, the GPF deformable model can effectively overcome image noise by enhancing the geometrical interaction field with a nonlocal edge-preserving algorithm. The vector force field introduced in this work is a generalised version of the magnetic force field described in the MAC model [Xie and Mirmehdi, 2008], but it can be extended to higher dimensions.

2.3.3 Variational segmentation models

Despite the many good numerical results based on the level set method, the widespread issue of the deformable modelling is related to the existence of local minima due to the non-convexity of its energy functional, which makes the choice of the initial condition critical to get satisfactory results. In this section, we provide an overview of variational techniques applied to deformable modelling due to their popularity in interactive segmentation, and approaches recently proposed to attain a global minimisation solution using convex relaxation. We also address their high potentials for making the real-time interactive medical segmentation become reality.

The active contour model (snakes) is one of the most successful variational deformable models in interactive segmentation. Following the first active contour model [Kass et al., 1988], Caselles et al. [Caselles et al., 1997] proposed the geodesic active contour (GAC) model, an enhanced snake model which is defined by the following minimisation problem:

$$\min_C \{E_{GAC}(C)\} = \min_C \left\{ \int_0^{L_C} g(|\nabla I(C(s))|) ds \right\}, \quad (1)$$

where I is the original image, C stands for the evolving contour (i.e., the boundary of the

evolving region in I), $L_C = \int_0^{L_C} ds$ denotes the Euclidean length of the curve C, and g is an edge indicator function (e.g., $g(|\nabla I|) = 1/(1+\beta|\nabla I|^2)$, β is a positive constant) that vanishes at object boundaries of I. The GAC energy function in (1) is actually a new length obtained by weighting the Euclidean element of length ds by the function g which contains information concerning the boundaries of objects.

In the GAC model, the existence of local minima in E_{GAC} can prevent the segmentation of meaningful objects in the images. Such a drawback necessitates the definition of a segmentation model that can provide correct results independently of the initial condition, i.e., a global minimum of a convex functional. In [Bresson et al., 2007], Bresson et al. proposed a fast global minimisation framework based on the unification of three variational models, namely the active contour model [Kass et al., 1988, Caselles et al., 1997], the Rudin-Osher-Fatemi (ROF) denoising model [Rudin et al., 1992] and the Mumford-Shah segmentation model [Mumford and Shah, 1989]. In the unified approach of image segmentation and ROF image denoising models, the convex energy functional is defined based on the dual formulation of the total variation (TV) norm [Chan et al., 1999, Chambolle, 2004, Aujol et al., 2006]:

$$\min_u \left\{ E_{TV_g}(u,\lambda) \right\} = \min_u \{ \underbrace{\int_\Omega g(x)|\nabla u| dx}_{TV_g(u)} + \lambda \int_\Omega |u-f| dx \}, \tag{2}$$

where Ω represents the image domain, u is a characteristic function, f is a given (possibly noisy) image, λ is a positive parameter controlling the scale of observation of the solution, and $TV_g(u)$ is the weighted total variation norm of the function u. The introduction of the weight function $g(x)$ in the TV-norm gives the link between the snakes/GAC model and the proposed functional $E_{TV_g}(u,\lambda)$. Bresson et al. [Bresson et al., 2007] proved that $E_{GAC}(C)$ in (1) and $E_{TV_g}(u)$ in (2) describe the same energy, when $g(x)$ is an edge indicator function, u is a characteristic function 1_{Ω_C} of a closed set $\Omega_C \subset \Omega$ whose boundary is denoted by C, and u is allowed to vary continuously in the interval $[0,1]$. The advantage of the energy functional defined in (2) over the one defined in (1) is its (non-strict) convexity, making it possible to derive a global optimal solution for u.

Applying the weighted TV minimisation algorithm [Bresson et al., 2007], Unger et al. [Unger et al., 2008] proposed the interactive TVSeg framework by minimising the following variational image segmentation model:

$$\min_{u\in[0,1]} \left\{ E_{TV_{Seg}}(u,\lambda(x)) \right\} = \min_{u\in[0,1]} \left\{ \int_\Omega g(x)|\nabla u| d\Omega + \int_\Omega \lambda(x)|u-f| d\Omega \right\}, \tag{3}$$

where $f \in [0,1]$ is provided by the user using the sampling brushes, indicating foreground ($f=1$) and background ($f=0$) seed regions. The spatially varying parameter $\lambda(x)$ is responsible for the interpretation of the information contained in f. The incorporation of different constraints (hard constraints: $\lambda(x) \to \infty$, weak constraints: $0<\lambda(x)<\infty$, and no constraints: $\lambda(x)=0$) enables the user to interact with the algorithm.

TVSeg is fast and easy to use, but exploits the colour histograms information only. To improve the segmentation quality, Santner et al. in [Santner et al., 2009] applied the Random Forests to learn the foreground and background labels from complex pixel descriptors consisting of colour, patch, and histograms of oriented gradients (HOGs) information. To regularise these labels for the final segmentation results, they employed a variational model

that combines the weighted TV-norm with a more flexible pointwise data term:

$$\min_{u\in[0,1]} \{E_p(u,\lambda)\} = \min_{u\in[0,1]} \{\underbrace{\int_\Omega g(x)|\nabla u| d\Omega}_{TV_g(u)} + \lambda \underbrace{\int_\Omega u f d\Omega}_{Region}\}, \tag{4}$$

where the weighting $g(\nabla I) = exp(-\alpha|\nabla I|^\beta)$ is an edge indicator function, u is the binary labelling results from the Random Forests classification, f is a function of probability (e.g., $f = \log(p_{bg}/p_{fg})$, a probability ratio of the background and foreground regions), and the positive parameter λ controls the influence of the TV_g term and the *Region* data term on the segmentation results. As shown in [Bresson et al., 2007], the energy functional in (4) becomes convex by letting u vary continuously between $[0,1]$. Compared with TVSeg, the simple product in the data term makes the global minimisation easier and faster. Using the recent primal-dual algorithms [Zhu et al., 2008, Zhu and Chan, 2008], a global optimal solution can be quickly obtained [Santner et al., 2009].

A great advantage of the above methods [Unger et al., 2008, Santner et al., 2009] is their high parallelisation potential. By implementing them on massively parallel processors such as the graphics processing unit (GPU), the real-time interactive segmentation becomes feasible, which is critical for the clinical applications.

2.4 Comparative studies

Medical images usually contain complex geometries and topologies, noise and weak edges. To generate good segmentation results, careful initialisation is commonly required. It is also worth noting that the method performs well on some particular dataset collected by a certain imaging technology (e.g., CT, MRI, or ultrasound) may not produce decent results on other datasets of the same or another imaging modality. In this section, we present a comparative evaluation of some interactive segmentation techniques discussed above with respect to their accuracy, given specific medical datasets and initialisation configurations.

As presented in Fig. 4, the segmentation results of the intelligent scissors (a fundamental approach) [Mortensen and Barrett, 1998] and the united snakes (a deformable model-based approach) [Liang et al., 2006] are compared on several medical images in terms of accuracy. We can see that with only a few seed points, the united snakes outperforms the intelligent scissors and its segmentation boundaries are comparable to the 'ideal' boundaries used as references in the intelligent scissors [Mortensen and Barrett, 1998].

In [He et al., 2008], various deformable contour methods were compared on representative images selected from several medical datasets including CT, MRI, ultrasound, and microscopy images. As an example of complex contour shape with deep concavities, sharp protrusions, and inhomogeneous interior intensities, seven initial contours (formed as circles around the user selected locations) were tried on a coronal MRI brain image. As depicted in Fig. 5a, the best result for the geodesic active contour (GAC) [Caselles et al., 1997] shows that GAC produces incomplete contour and it cannot acquire small sharp protrusions in the contour segments at the lower left and right sides of the brain. Applying the same method to another MRI brain image containing weak edges and complex topologies with acute concavities, it steps across the weak edges but fails to localise the boundaries (see Fig. 5d), with the initialisation across both the left and right hemispheres. With two initial surfaces being placed inside the object of interest, the GAC model usually cannot propagate through

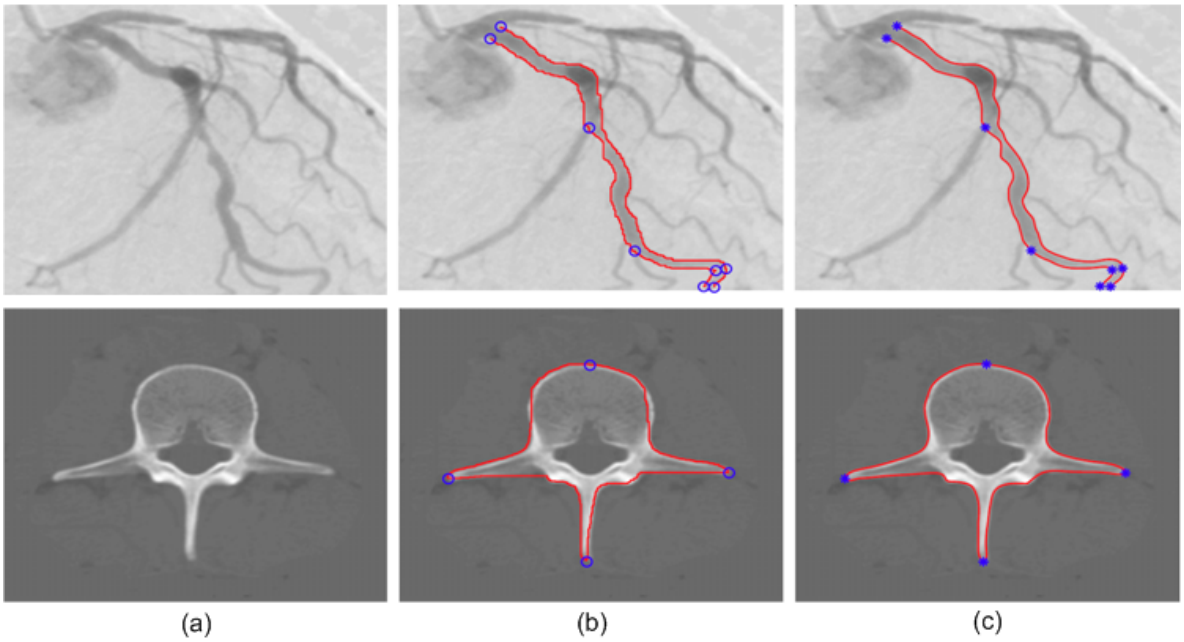

Figure 4: Segmentation results on angiogram of coronary artery (top row) and CT scan of spinal vertebrae (bottom row) [Liang et al., 2006]. (a) The ground truth images [Mortensen and Barrett, 1998], (b) intelligent scissors segmentation, and (c) united snakes segmentation.

the narrow tubular structures in the 3D MRI cerebral artery image and leaks out at weak object boundaries during the evolution (see Fig. 5g). As shown in Fig. 5b, the generalized gradient vector flow (GGVF) [Xu and Prince, 1998a] method can extract the endocardial border and also the papillary muscle protruding into the cavity in the MRI image (short-axis section) of the left ventricle of a human heart, where the circle is the initial position for GGVF active contour. However, using the same initialisation as in Fig. 5d, GGVF fails to evolve through the tortuous structures and collapses to nearby edges (see Fig. 5e). By placing two initial surfaces across the object boundaries, the GGVF model again collapses to the nearby object edges owing to the saddle or stationary points inside the narrow image structures (see Fig. 5h). In contrast, the constrained optimisation [Wang et al., 2004] approach yields the best qualitative result (see Fig. 5c), as it considers both edge and region features. In Fig. 5f, the magnetostatic active contour (MAC) [Xie and Mirmehdi, 2008] model successfully evolves through the narrow and twisted structures, and in Fig. 5i, the geometric potential force (GPF) [Yeo et al., 2011] model is able to propagate through the long tubular structures to extract the cerebral arterial geometry, despite the noise, weak edges, and inhomogeneous intensities present in the image. Note that these good results are achieved with the same initialisations as those in Fig. 5a,d,h, respectively.

In summary, the interactive segmentation results rely extensively on the medical datasets and user initialisations one way or the other. Generally, the variation in initialisation configurations will result in different results, as illustrated in Fig. 6a,b [Siddiqi et al., 1998]. However, this may not always be true for all the segmentation techniques. For some learning-based approaches (e.g., Bayesian Transductive learning [Lee et al., 2009]), the user only needs to initialise a single or a few slice images in the volume. The initialisations for other slices will be predicted by learning the user intention (see Fig. 6c,d). In [Xie, 2010], Xie presented an edge-based active contour model with high initialisation flexibility, as its dynamic force

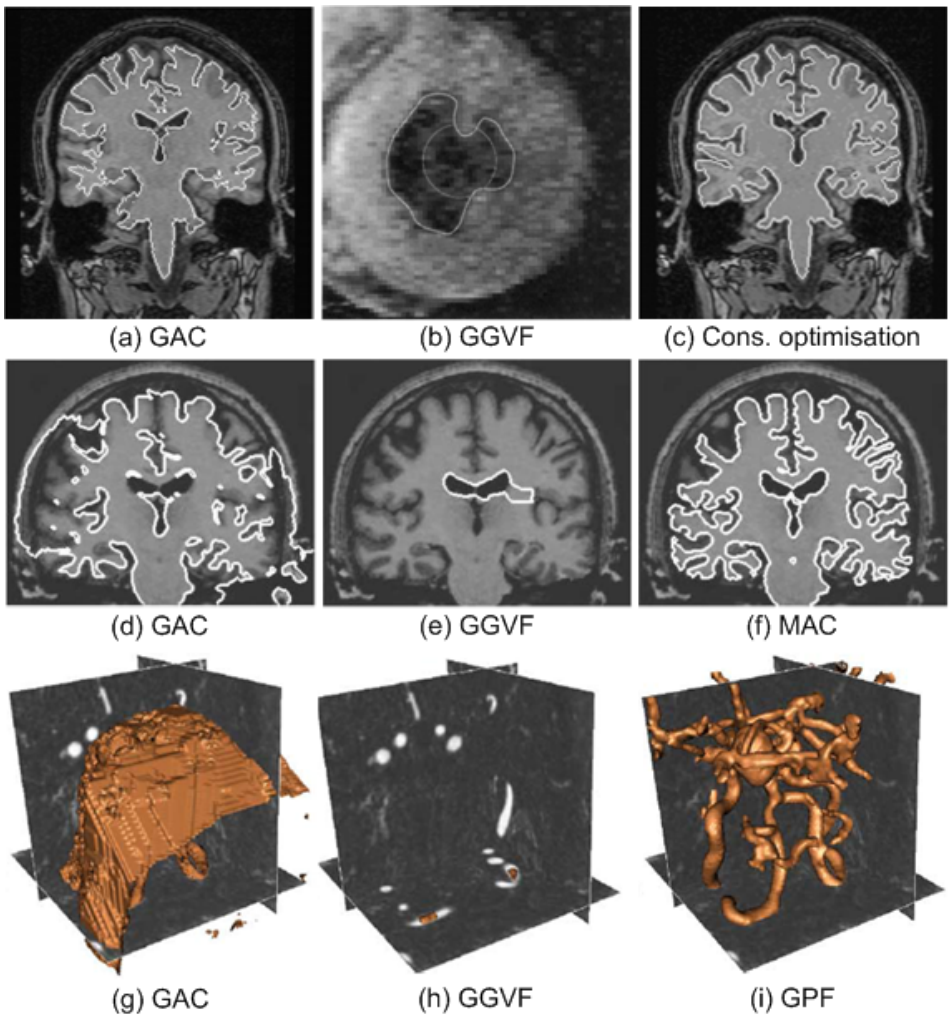

Figure 5: Segmentation results on MRI images of the (a,c) brain [He et al., 2008], (b) left ventricle [Xu and Prince, 1998a], (d-f) brain [Xie and Mirmehdi, 2008], and (g-i) cerebral artery [Yeo et al., 2011] using different methods: GAC [Caselles et al., 1997], GGVF [Xu and Prince, 1998a], constrained optimisation [Wang et al., 2004], (MAC) [Xie and Mirmehdi, 2008], and GPF [Yeo et al., 2011].

field, unique bidirectionality, and constrained diffusion-based level set evolution provide great freedom in contour initialisation. As shown in Fig. 6e-g, no discernable difference can be seen from the segmentation results under three completely different initialisations.

3 Interactions in Medical Image Segmentation

In an interactive segmentation framework, user intervention is tightly coupled with an automatic segmentation algorithm leveraging the user's high-level anatomical knowledge and the automated method's computational capability. Real-time visualisation on the screen enables the user to quickly validate and correct the automatic segmentation results in a subdomain where the variational model's statistical assumptions do not agree with the user's expert knowledge. The user intervention mainly includes initialisation of the methods,

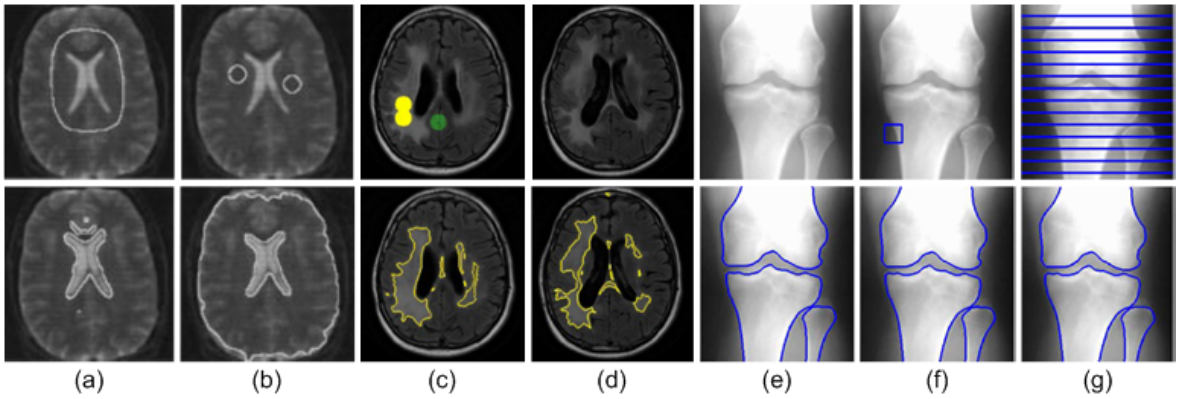

Figure 6: Segmentation results (bottom row) under different initial conditions (top row). (a)(b) MRI brain ventricle extraction under two entirely different initialisation methods [Siddiqi et al., 1998], (c)(d) MRI brain edema segmentation with and without initialisation [Lee et al., 2009], and (e)-(g) CT bone segmentation with no initial contour, cross boundary initialisation, and horizontal lines, respectively [Xie, 2010].

checking the accuracy of the results produced by automatic segmentation, and corrections to the segmentation results using specialised interactive segmentation tools. As shown in Table 1, interactions in the segmentation of medical images can be broadly classified into three types: pictorial input on an image grid, parameter tuning, and menu option selection. The segmentation results obtained with new configurations (e.g., mouse clicking/drawing, new parameter values, another menu option) are visualised on the screen in real time for further user evaluation. Among all the three types of user interactions, menu option selection is most efficient, but it constrains the degrees of freedom for the user's choice to selections. Pictorial input is simple, but it could be time-consuming in case the interaction requires a user to draw precisely on an image grid. Parameter tuning is easy to operate, but it may require specific training for an insight into the automatic computational part.

Interactive segmentation techniques are very important for fast and reliable extraction of the regions of interest. The level of user interaction in different methods varies in terms of the amount and type of information provided by the users. Their underlying mathematical framework is a significant factor determining the form of interaction. In region growing-based methods [Adams and Bischof, 1994, Wu et al., 2008b], the interaction is the selection of initial seed points. In the united snakes framework [Liang et al., 2006], the user controls the snake evolution by 'planting' seed points. The GrabCut technique [Rother et al., 2004] is based on the discrete graph-cut approach, where image pixels represent graph vertices. The partitioning of the image into object and background regions is obtained by solving the min-cut problem in graphs. The user controls the segmentation by labelling regions, which are correspondingly assigned to either the source or the sink of the graph. The selected regions provide colour statistics that characterise the object and the background and are utilised for segmentation. In [Paragios, 2004], Paragios presented a semi-automatic segmentation of the left ventricle. The method uses linear or quadratic interpolation to convert the user input into closed structures. Therefore, the feedback is not part of the level set formulation. In [Li et al., 2006a], a method applying dual-front active contours and active regions for 3D cortical segmentation is proposed. The user can modify the initialisation of the active region by adding or deleting labels. A probabilistic level-set method which supports user interaction

Interactions in Medical Image Segmentation	Examples
Pictorial input (points, lines, or regions) on an image grid	Points of background and objects [Griffin et al., 1994, Higgins et al., 1994, Maes, 1998, Santner et al., 2009] Seeds for region growing [Adams and Bischof, 1994, Wu et al., 2008b] Point of object for initiating an inflating 3D balloon [Gill et al., 1999] Centre point and radius [Bzostek et al., 1998] Rectangles indicating regions of interest [Lifshitz and Pizer, 1990, Santner et al., 2009] Features of different types of objects [Udupa et al., 1997] Points attracting/repelling the contour [Kass et al., 1988, Caselles et al., 1993, Eviatar and Somorjai, 1996] Initial curve/surface of objects of interest [McInerney and Terzopoulos, 1996]
Parameter tuning using slider, dial, or similar interface	Scale for computing image derivatives [Lifshitz and Pizer, 1990, Cabral et al., 1993] Balance of weights in the cost function [Buck et al., 1995] Maximum number of iterations [Cabral et al., 1993] Maximum size of segmented regions [Sivewright and Elliot, 1994]
Menu option selection by mouse clicking	Accept/reject the segmentation results [Udupa et al., 1997] Type of geometry model [Buck et al., 1995, Hinshaw et al., 1995] Properties of objects of interest [Higgins et al., 1994]

Table 1: Type of interactions in the segmentation of medical images.

is demonstrated in [Cremers et al., 2007a]. The user-labelled input points are viewed as independent measurements of the scene. In [Ben-Zadok et al., 2009], Ben-Zadok et al. developed a novel active-contour segmentation framework, which supports an intuitive and friendly user interaction subject to the 'bottom up' constraints introduced by the image features. Applying the level-set method [Osher and Sethian, 1988], a fully automatic segmentation is first obtained by minimising a cost functional that is uniquely based on the image data. The user does not 'edit' the initial segmentation, but influences its evolution with a few mouse clicks located in regions of 'disagreement'. The user input is represented as a continuous energy term that is incorporated into the primary level-set cost functional. This additional term affects the gradient descent process by attracting it toward a new local minimum, which results in a modified segmentation consistent with both the low-level image data and the top-down user feedback points. In [Santner et al., 2009], it allows the user to intervene the segmentation by adding foreground/background pixels to the Random Forests training set with brush strokes or drawing a rectangle over the object of interest and then randomly sampling pixels inside and outside the rectangle as the training set.

4 Performance Evaluation

Many interactive segmentation methods have been widely applied for various medical imaging modalities such as CT, MRI, and Ultrasound. Since these methods use different strategies to combine the prior-knowledge of users with automatic segmentation, the performance of such methods depends on both the interaction strategy and automatic computation. Accordingly, a good evaluation of interactive segmentation methods requires an equal understanding of the interactive and computational parts. In the early literature, the capabilities of

interactive segmentation methods can be demonstrated in terms of accuracy, efficiency, and repeatability [Olabarriaga and Smeulders, 2001]. These criteria are highly related, particularly accuracy and efficiency are interdependent since a user usually produce more accurate segmentation results given more time. Meanwhile, it is important to note that the performance evaluation may be considered reasonable for one application but not acceptable for another.

Accuracy is the most common criterion for performance evaluation, indicating the degree of similarity between the segmentation results and their respective ground truth. It can be assessed subjectively by a human expert by ranking the results [Udupa et al., 1997] or objectively by comparing the results with the ground truth using different distance measures [de Graaf et al., 1992, Chalana and Kim, 1997, Bello and Colchester, 1998]. The ground truth adopted is a golden standard usually generated by a human expert using manual segmentation tools. Due to manual processing, the golden standard may incorporate variation and subjectivity, which should be taken into account in the global evaluation of accuracy.

Efficiency of an interactive segmentation can be assessed with respect to the total computation time [Mortensen and Barrett, 1998] or the amount of user's effort to complete the segmentation task. This effort is determined mostly by the amount and the nature of user interactions. The amount of interaction is often estimated in terms of the number of mouse clicks [Vehkomäi et al., 1997, Bzostek et al., 1998], while the nature of interaction correlates to the complexity of the task performed by the user [Hastreiter and Ertl, 1998, Mortensen and Barrett, 1998]. Task complexity involves several issues, including the effort to accomplish required mouse operation, the type of knowledge needed to input data during interaction, and the predictability of the impact of user input. It is reasonable to conclude that the efficiency of a method is high if the computational part is fast, highly autonomous and predictable, and the user interaction is simple, few and quick.

Repeatability is to evaluate the extent to which the same result can be generated in different segmentation sessions with the same user intention. In such a case, the same objects of interest are segmented several times by a user (intra-operator) and the results are compared. The same procedure is followed to assess the inter-operator repeatability. The differences indicate the intra-operator or inter-operator variability of results [Udupa et al., 1997, Mortensen and Barrett, 1998, Gill et al., 1999].

In [McGuinness and O'Connor, 2010], McGuinness and O'Connor presented a comparative evaluation of four popular interactive segmentation algorithms: seeded region growing [Adams and Bischof, 1994], interactive graph cuts [Boykov and Jolly, 2001], simple interactive object extraction [Friedland et al., 2005], and interactive segmentation using binary partition trees [Salembier and Garrido, 2000]. In a series of user-experiments, the participants were asked to extract 100 objects using different interactive segmentation algorithms by simply marking areas of foreground and background with a mouse, constrained within a time limit of 2 minutes for each object. The updated segmentation masks were stored along with the elapsed time after each participant performed a new interaction. Every recorded mask was evaluated against the corresponding manually segmented ground truth to measure the average segmentation accuracy over time, using two benchmarks: the well-known Jaccard index [Ge et al., 2007] for measuring object accuracy, and the proposed fuzzy metric [McGuinness and O'Connor, 2010] for measuring boundary accuracy. As reported in [McGuinness and O'Connor, 2010], the overall average boundary and object accuracies of the interactive graph cuts and the binary partition trees are higher than those of the other two methods.

It is worth noting that quantitative assessment is generally difficult for real medical images, as they contain complex anatomical structures and the manual segmentation by a human expert may be unavailable. Mostly, qualitative results are provided instead.

5 Conclusions

In this paper, we review the interactive image segmentation techniques that are widely used in many medical applications. This review gives us some insights into the state-of-the-art segmentations and user interventions. Even though the research on interactive segmentation is expanding rapidly, there are still many challenges to be faced. Based on this review, we make the following observations.

1. Interactive segmentation takes advantage of automatic segmentation and allows users to intervene the segmentation process, which are very important for fast and reliable medical image segmentation.

2. User intervention (e.g., initialisation, validating results, correcting errors) provides additional source of information for image segmentation, thus potentially produces accurate segmentation results.

3. A significant amount of reported works are based on energy minimisation, especially the variational deformable modelling approaches. Specific parameter tuning and/or careful initialisation are usually involved in these methods. Their segmentation accuracy and efficiency may vary on different datasets and also rely on the initialisation configurations. Techniques that can efficiently segment anatomical structures with high accuracy are still a challenge for interactive medical image segmentation. A good thing is that these methods are not mutually exclusive, so they can be incorporated to handle practical problems.

4. The desired object boundary might be unclear or even missing in many medical images. Thus, it is important to impose soft or hard constraints to capture the intricate details and bridge gaps along object boundaries in practical image segmentation.

5. Interactive segmentation aims to achieve interaction efficiency by incorporating intelligence with automatic segmentation, leading to the ability of learning user intention and dealing with new volumetric images. A possible direction for future work could be how to efficiently learn the intention of the user so as to reduce the number of user interactions.

6. To be viable for practical applications, an interactive segmentation approach should (i) minimise user interaction, (ii) minimise segmentation variability among users and (iii) be computationally fast to allow quick user editing. These concerns can be addressed by combining the machine learning techniques with interactive segmentation algorithms. Such a combined approach could provide a promising direction for accurate segmentation of medical images.

7. Real-time interactive segmentation of multimodal volumetric medical images is highly desirable for clinical applications. Owing to the advancement in high performance computing such as GPU, the real-time response becomes feasible. Thus, algorithms

with high parallelisation potential that can be easily implemented on the GPU are desirable.

8. There is a clear need of some benchmark medical datasets and well-defined performance evaluation protocols for comparative studies.

References

R. Adams and L. Bischof. Seeded region growing. *IEEE Trans. Pattern Anal. Mach. Intell.*, 16 (6):641–647, 1994.

C. J. Armstrong, B. L. Price, and W. A. Barrett. Interactive segmentation of image volumes with live surface. *Computers & Graphics*, 31(2):212–229, 2007.

J. F. Aujol, G. Gilboa, T. Chan, and S. Osher. Structure-texture image decomposition - modeling, algorithms, and parameter selection. *Int. J. Comput. Vis.*, 67(1):111–136, 2006.

C. Baillard and C. Barillot. Robust 3D segmentation of anatomical structures with level sets. In *Proc. Int. Conf. Medical Image Computing and Computer Assisted Intervention*, pages 236–245, 2000.

F. Bello and A. C. F. Colchester. Measuring global and local spatial correspondence using information theory. In *Proc. Int. Conf. Medical Image Computing and Computer Assisted Intervention*, pages 964–973, 1998.

N. Ben-Zadok, T. Riklin-Raviv, and N. Kiryati. Interactive level set segmentation for image-guided therapy. In *Proc. Int. Sym. Biomedical Imaging: From Nano to Macro*, pages 1079–1082, 2009.

B. Bhanu and S. Fonder. Learning based interactive image segmentation. In *Proc. Int. Conf. Pattern Recognit.*, pages 299–302, 2000.

Y. Boykov and M. P. Jolly. Interactive graph cuts for optimal boundary and region segmentation of objects in N-D images. In *Proc. IEEE Int. Conf. Comput. Vis.*, pages 105–112, 2001.

J. Bredno, T. M. Lehmann, and K. Spitzer. A general discrete contour model in two, three, and four dimensions for topology-adaptive multichannel segmentation. *IEEE Trans. Pattern Anal. Mach. Intell.*, 25(5):550–563, May 2003.

L. Breiman. Random forests. *Machine Learning*, 45:5–32, 2001.

X. Bresson, S. Esedoglu, P. Vandergheynst, J. P. Thiran, and S. J. Osher. Fast global minimization of the active contour/snake model. *J. Math. Imaging Vis.*, 28(2):151–167, 2007.

T. A. Buck, H. H. Ehricke, W. Strasser, and L. Thurfjel. 3D segmentation of medical structures by integration of ray-casting with anatomic knowledge. *Computers & Graphics*, 19(3):441–449, 1995.

A. Bzostek, G. Ionescu, L. Carrat, C. Barbe, O. Chavanon, and J. Troccaz. Isolating moving anatomy in ultrasound without anatomical knowledge: Application to computer-assisted pericardial punctures. In *Proc. Int. Conf. Medical Image Computing and Computer Assisted Intervention*, pages 1041–1048, 1998.

J. E. Cabral, K. S. White, Y. Kim, and E. L. Effmann. Interactive segmentation of brain tumors in MR images using 3D region-growing. In *Proc. SPIE Conf. Medical Imaging*, pages 171–181, 1993.

S. Cagnoni, A. B. Dobrzeniecki, R. Poli, and J. C. Yanch. Genetic algorithm-based interactive segmentation of 3D medical images. *Image and Vision Computing*, 17(12):881–895, 1999.

V. Caselles, F. Catte, T. Coll, and F. Dibos. A geometric model for active contours in image processing. *Numer. Math.*, 66(1):1–31, 1993.

V. Caselles, R. Kimmel, and G. Sapiro. Geodesic active contours. *Int. J. Comput. Vis.*, 22(1): 61–79, 1997.

V. Chalana and Y. Kim. A methodology for evaluation of boundary detection algorithms on medical images. *IEEE Trans. Med. Imag.*, 16(5):642–652, 1997.

A. Chambolle. An algorithm for total variation minimization and applications. *J. Math. Imaging Vis.*, 20(1-2):89–97, 2004.

T. Chan and L. Vese. Active contours without edges. *IEEE Trans. Image Process.*, 10(2):266–277, Feb. 2001.

T. Chan, G. Golub, and P. Mulet. A nonlinear primal-dual method for total variation-based image restoration. *SIAM J. Sci. Comput.*, 20(6):1964–1977, 1999.

A. C. S. Chung and J. A. Noble. Statistical 3D vessel segmentation using a Rician distribution. In *Proc. Int. Conf. Medical Image Computing and Computer Assisted Intervention*, pages 82–89, 1999.

D. Cremers, O. Fluck, M. Rousson, and S. Aharon. A probabilistic level set formulation for interactive organ segmentation. In *Proc. SPIE Medical Imaging*, 2007a.

D. Cremers, M. Rousson, and R. Deriche. A review of statistical approaches to level set segmentation: Integrating color, texture, motion and shape. *Int. J. Comput. Vis.*, 72(2):195–215, 2007b.

C. N. de Graaf, A. S. E. Koster, K. L. Vincken, and M. A. Viergever. A methodology for the validation of image segmentation methods. In *Proc. Annual Sym. Computer-Based Medical Systems*, pages 17–24, 1992.

H. Delingette and J. Montagnat. Shape and topology constraints on parametric active contours. *J. Comput. Vis. Image Understand.*, 83(2):140–171, 2001.

S. Diciotti, S. Lombardo, M. Falchini, G. Picozzi, and M. Mascalchi. Automated segmentation refinement of small lung nodules in CT scans by local shape analysis. *IEEE Trans. Biomed. Eng.*, 58(12):3418–3428, 2011.

P. J. Elliot, J. M. Knapman, and W. Schlegel. Interactive image segmentation for radiation treatment planning. *IBM Systems Journal*, 31(4):620–634, 1992.

H. Eviatar and R. L. Somorjai. A fast simple active contour algorithm for biomedical images. *Pattern Recognition Letters*, 17:969–974, 1996.

G. Friedland, K. Jantz, and R. Rojas. SIOX: Simple interactive object extraction in still images. In *Proc. IEEE Int. Sym. Multimedia*, pages 253–260, 2005.

F. Ge, S. Wang, and T. Liu. New benchmark for image segmentation evaluation. *J. Electronic Imaging*, 16(3):033011, 2007.

J. D. Gill, H. M. Ladak, D. A. Steinman, and A. Fenster. Development and evaluation of a semi-automatic 3D segmentation of the carotid arteries from 3D ultrasound images. In *Proc. SPIE Conf. Medical Imaging*, pages 214–221, 1999.

V. Grau, A. U. J. Mewes, M. Alcaniz, R. Kikinis, and S. K. Warfield. Improved watershed transform for medical image segmentation using prior information. *IEEE Trans. Med. Imag.*, 23(4):447–458, Apr. 2004.

L. D. Griffin, A. C. F. Colchester, S. A. Röll, and C. S. Studholme. Hierarchical segmentation satisfying constraints. In *Proc. British Mach. Vis. Conf.*, pages 135–144, 1994.

M. W. Hansen and W. E. Higgins. Relaxation methods for supervised image segmentation. *IEEE Trans. Pattern Anal. Mach. Intell.*, 19(9):949–962, 1997.

J. Hao and M. Li. A supervised bayesian method for cerebrovascular segmentation. *WSEAS Trans. Signal Process.*, 3(12):487–495, 2007.

P. Hastreiter and T. Ertl. Fast and interactive 3D segmentation of medical volume data. In *Proc. Conf. Image and Multi-dimensional Digital Signal Processing*, pages 41–44, 1998.

L. He, Z. Peng, B. Everding, X. Wang, C. Y. Han, K. L. Weiss, and W. G. Wee. A comparative study of deformable contour methods on medical image segmentation. *Image and Vision Computing*, 26(2):141–163, 2008.

W. E. Higgins, J. M. Reinhardt, and W. L. Sharp. Semi-automatic construction of 3D medical image-segmentation processes. In *Proc. SPIE Conf. Visualization in Biomedical Computing*, pages 59–71, 1994.

K. P. Hinshaw, R. B. Altman, and J. F. Brinkley. Shape-based models for interactive segmentation of medical images. In *Proc. SPIE Conf. Medical Imaging*, pages 771–780, 1995.

M. Holtzman-Gazit, R. Kimmel, N. Peled, and D. Goldsher. Segmentation of thin structures in volumetric medical images. *IEEE Trans. Image Process.*, 15(2):354–363, Feb. 2006.

M. Kass, A. Witkin, and D. Terzopoulos. Snakes: Active contour models. *Int. J. Comput. Vis.*, 1(4):321–331, 1988.

J. Kim, J. W. Fisher, A. Yezzi, M. Cetin, and A. S. Willsky. A nonparametric statistical method for image segmentation using information theory and curve evolution. *IEEE Trans. Image Process.*, 14(10):1486–1502, Oct. 2005.

R. Kimmel. *Geometric Level Set Methods in Imaging, Vision, and Graphics*, chapter Fast edge integration, pages 59–77. Berlin, Germany: Springer-Verlag, 2003.

T. Kubota, A. K. Jerebko, M. Dewan, M. Salganicoff, and A. Krishnan. Segmentation of pulmonary nodules of various densities with morphological approaches and convexity models. *Medical Image Analysis*, 15(1):133–154, 2011.

J.-O. Lauchaud and B. Taton. Deformable model with a complexity independent from image resolution. *J. Comput. Vis. Image Understand.*, 99(3):453–475, 2005.

M. Law and A. Chung. A deformable surface model for vascular segmentation. In *Proc. Int. Conf. Medical Image Computing and Computer Assisted Intervention*, pages 59–67, 2009.

N. Lee, R. T. Smith, and A. F. Laine. Interactive segmentation for geographic atrophy in retinal fundus images. In *Proc. 42nd Asilomar Conf. Signals, Systems and Computers*, pages 655–658, 2008.

N. Lee, J. Caban, S. Ebadollahi, and A. Laine. Interactive segmentation in multimodal medical imagery using a bayesian transductive learning approach. In *Proc. Medical Imaging: Computer-Aided Diagnosis*, pages 72601W–1–10, 2009.

C. Li, J. Liu, and M. Fox. Segmentation of edge preserving gradient vector flow: An approach toward automatically initializing and splitting of snakes. In *Proc. IEEE Conf. Comput. Vis. Pattern Recognit.*, pages 162–167, 2005.

H. Li, A. Yezzi, and L. D. Cohen. 3D brain segmentation using dual-front active contours with optional user interaction. *Int. J. Biomedical Imaging*, 2006:1–17, 2006a.

K. Li, X. Wu, D. Z. Chen, and M. Sonka. Optimal surface segmentation in volumetric images-A graph-theoretic approach. *IEEE Trans. Pattern Anal. Mach. Intell.*, 28(1):119–134, 2006b.

Y. Li, J. Sun, C.-K. Tang, and H.-Y. Shum. Lazy snapping. In *Proc. ACM SIGGRAPH*, pages 303–308, 2004.

J. Liang, T. McInerney, and D. Terzopoulos. United snakes. *Medical Image Analysis*, 10(2): 215–233, 2006.

L. M. Lifshitz and S. M. Pizer. Multiresolution hierarchical approach to image segmentation based on intensity extrema. *IEEE Trans. Pattern Anal. Mach. Intell.*, 12(6):529–540, 1990.

H. Lombaert, Y. Sun, L. Grady, and C. Xu. A multilevel banded graph cuts method for fast image segmentation. In *Proc. IEEE Int. Conf. Comput. Vis.*, pages 259–265, 2005.

F. Maes. *Segmentation and registration of multimodal images: From theory, implementation and validation to a useful tool in clinical practice*. PhD thesis, Katholieke Universiteit Leuven, Leuven, BE., 1998.

R. Malladi, J. A. Sethian, and B. C. Vemuri. Shape modeling with front propagation: A level set approach. *IEEE Trans. Pattern Anal. Mach. Intell.*, 17(2):158–175, Feb. 1995.

K. McGuinness and N. E. O'Connor. A comparative evaluation of interactive segmentation algorithms. *Pattern Recognition*, 43(2):434–444, 2010.

T. McInerney and D. Terzopoulos. Deformable models in medical image analysis: A survey. *Medical Image Analysis*, 1(2):91–108, 1996.

T. McInerney and D. Terzopoulos. Topology adaptive deformable surfaces for medical image volume segmentation. *IEEE Trans. Med. Imag.*, 18(10):840–850, Oct. 1999.

T. Mondal, A. Jain, and H. K. Sardana. Automatic craniofacial structure detection on cephalometric images. *IEEE Trans. Image Process.*, 20(9):2606–2614, 2011.

E. N. Mortensen and W. A. Barrett. Interactive segmentation with intelligent scissors. *Graphical Models and Image Processing*, 60(5):349–384, 1998.

D. Mumford and J. Shah. Optimal approximations of piecewise smooth functions and associated variational problems. *Commun. Pure Appl. Math.*, 42(5):577–685, 1989.

S. D. Olabarriaga and A. W. M Smeulders. Setting the mind for intelligent interactive segmentation: Overview, requirements, and framework. In *Proc. Int. Conf. Information Processing in Medical Imaging*, pages 417–422, 1997.

S. D. Olabarriaga and A. W. M. Smeulders. Interaction in the segmentation of medical images: A survey. *Medical Image Analysis*, 5(2):127–142, 2001.

J. Olivier, C. Mocquillon, J. J. Rousselle, R. Boné, and H. Cardot. A supervised texture-based active contour model with linear programming. In *Proc. IEEE Int. Conf. Image Processing*, pages 1104–1107, 2008.

S. J. Osher and J. A. Sethian. Fronts propagation with curvature dependent speed: Algorithms based on Hamilton-Jacobi formulations. *J. Comp. Phys.*, 79:12–49, 1988.

N. Paragios. Variational methods and partial differential equations in cardiac image analysis. In *Proc. Int. Sym. Biomedical Imaging: From Nano to Macro*, pages 17–20, 2004.

N. Paragios and R. Deriche. Geodesic active regions and level set methods for supervised texture segmentation. *Int. J. Comput. Vis.*, 46(3):223–247, 2002.

N. Paragios, O. Mellina-Gottardo, and V. Ramesh. Gradient vector flow geometric active contours. *IEEE Trans. Pattern Anal. Mach. Intell.*, 26(3):402–407, 2004.

A. Pitiot, A. W. Toga, N. Ayache, and P. Thompson. Texture based MRI segmentation with a two-stage hybrid neural classifier. In *Proc. World Congress Computational Intelligence/INNS-IEEE Int. Joint Conf. Neural Networks*, pages 2053–2058, 2002.

L. J. Reese and W. A. Barrett. Image editing with intelligent paint. In *Proc. Eurographics*, pages 714–724, 2002.

C. C. Reyes-Aldasoro and A. Bhalerao. Volumetric texture segmentation by discriminant feature selection and multiresolution classification. *IEEE Trans. Med. Imag.*, 26(1):1–14, Jan. 2007.

C. Rother, V. Kolmogorov, and A. Blake. Grabcut - Interactive foreground extraction using iterated graph cuts. In *Proc. ACM SIGGRAPH*, pages 309–314, 2004.

L. I. Rudin, S. Osher, and E. Fatemi. Nonlinear total variation based noise removal algorithms. *Phys. D*, 60(1-4):259–268, 1992.

A. Saffari, C. Leistner, J. Santner, M. Godec, and H. Bischof. On-line random forests. In *Proc. ICCV Workshop On-line Computer Vision*, pages 1393–1400, 2009.

P. Salembier and L. Garrido. Binary partition tree as an effcient representation for image processing, segmentation, and information retrieval. *IEEE Trans. Image Process.*, 9(4):561–576, 2000.

J. Santner, M. Unger, T. Pock, C. Leistner, A. Saffari, and H. Bischof. Interactive texture segmentation using random forests and total variation. In *Proc. British Mach. Vis. Conf.*, 2009.

M. Schaap, T. van Walsum, L. Neefjes, C. Metz, E. Capuano, M. de Bruijne, and W. Niessen. Robust shape regression for supervised vessel segmentation and its application to coronary segmentation in CTA. *IEEE Trans. Med. Imag.*, 30(11):1974–1986, 2011.

J. A. Sethian. *Level Set Methods and Fast Marching Methods: Evolving Interfaces in Computational Geometry, Fluid Mechanics, Computer Vision, and Material Science*. Cambridge University Press, 1999.

J. Shi and J. Malik. Normalized cuts and image segmentation. *IEEE Trans. Pattern Anal. Mach. Intell.*, 22(8):888–905, Aug. 2000.

K. Siddiqi, Y. Lauzière, A. Tannenbaum, and S. Zucker. Area and length minimizing flows for shape segmentation. *IEEE Trans. Image Process.*, 7(3):433–443, 1998.

J. Sijbers, A. Van der Linden, P. Scheunders, J. Van Audekerke, D. Van Dyck, and E. Raman. Volume quantization of the mouse cerebellum by semi-automatic 3D segmentation of magnetic resonance images. In *SPIE Conf. Medical Imaging*, pages 553–560, 1996.

G. J. Sivewright and P. J. Elliot. Interactive region and volume growing for segmenting volumes in MR and CT images. *Medical informatics*, 19(1):71–80, 1994.

A. W. M. Smeulders, S. D. Olabarriaga, R. Van den Boomgaard, and M. Worring. Design considerations for interactive segmentation. In *Proc. Conf. Visual Information Systems*, pages 5–12, 1997.

C. M. Smith, J. Smith, S. K. Williams, J. J. Rodriguez, and J. B. Hoying. Automatic thresholding of three-dimensional microvascular structures from confocal microscopy images. *J. Microscopy*, 225(3):244–257, 2007.

J. K. Udupa, L. Wei, S. Samarasekera, Y. Miki, M. A. van Buchem, and R. I. Grossman. Multiple sclerosis lesion quantification using fuzzy-connectedness principles. *IEEE Trans. Med. Imag.*, 16(5):598–609, 1997.

M. Unger, T. Pock, W. Trobin, D. Cremers, and H. Bischof. TVSeg - Interactive total variation based image segmentation. In *Proc. British Mach. Vis. Conf.*, 2008.

H. Veeraraghavan and J. V. Miller. Active learning guided interactions for consistent image segmentation with reduced user interactions. In *Proc. Int. Sym. Biomedical Imaging: From Nano to Macro*, pages 1645–1648, 2011.

T. Vehkomäi, G. Gerig, and G. Székely. A user-guided tool for efficient segmentation of medical data. In *Proc. Conf. Computer Vision, Virtual Reality and Robotics in Medicine and Medical Robotics and Computer-Assisted Surgery*, pages 685–694, 1997.

L. Vese and T. Chan. A multiphase level set framework for image segmentation using the mumford and shah model. *Int. J. Comput. Vis.*, 50(3):271–293, 2002.

X. Wang, L. He, and W. G. Wee. Deformable contour method: A constrained optimization approach. *Int. J. Comput. Vis.*, 59(1):87–108, 2004.

O. Wink, K. J. Zuiderveld, and M. A. Viergever. Interactive volume segmentation using local similarity measurements. In *Proc. Computer Assisted Radiology Conf.*, page 996, 1997.

J. Wu, S. Poehlman, M. D. Noseworthy, and M. V. Kamath. Texture feature based automated seeded region growing in abdominal MRI segmentation. In *Proc. Int. Conf. BioMedical Engineering and Informatics*, volume 2, pages 263–267, 2008a.

J. Wu, F. Ye, J. Ma, X. Sun, J. Xu, and Z. Cui. The segmentation and visualization of human organs based on adaptive region growing method. In *Proc. Int. Conf. Comp. Inf. Tech.*, pages 439–443, 2008b.

X. Xie. Active contouring based on gradient vector interaction and constrained level set diffusion. *IEEE Trans. Image Process.*, 19(1):154–164, 2010.

X. Xie and M. Mirmehdi. RAGS: Region-aided geometric snake. *IEEE Trans. Image Process.*, 13(5):640–652, May 2004.

X. Xie and M. Mirmehdi. MAC: Magnetostatic active contour model. *IEEE Trans. Pattern Anal. Mach. Intell.*, 30(4):632–647, 2008.

C. Xu and J. L. Prince. Generalized gradient vector flow external forces for active contours. *Signal Process.*, 71(2):131–139, 1998a.

C. Xu and J. L. Prince. Snakes, shapes, and gradient vector flow. *IEEE Trans. Image Process.*, 7(3):359–369, Mar. 1998b.

S. Y. Yeo, X. Xie, I. Sazonov, and P. Nithiarasu. Geometrically induced force interaction for three-dimensional deformable models. *IEEE Trans. Image Process.*, 20(5):1373–1387, May 2011.

X. Yu and J. Yla-Jaaski. Interactive surface segmentation for medical images. In *Proc. Int. Conf. Signal Processing*, pages 1178–1181, 1996.

X. Yuan, N. Zhang, M. X. Nguyen, and B. Chen. Volume cutout. *Visual Computer (Special Issue of Pacific Graphics)*, 21(8-10):745–754, 2005.

M. Zhu and T. Chan. An efficient primal-dual hybrid gradient algorithm for total variation image restoration. Technical Report 08-34, UCLA CAM, 2008.

M. Zhu, S. Wright, and T. Chan. Duality-based algorithms for total-variation-regularized image restoration. Technical Report 08-33, UCLA CAM, 2008.